

## Biostimulated uranium immobilization within aquifers – from bench scale to field experiments

Kai-Uwe Ulrich<sup>1,4</sup>, Harish Veeramani<sup>2,7</sup>, Eleanor J. Schofield<sup>3,8</sup>, Jonathan O. Sharp<sup>2,9</sup>, Elena I. Suvorova<sup>2</sup>, Joanne E. Stubbs<sup>3</sup>, Juan S. Lezama-Pacheco<sup>3</sup>, Charles J. Barrows<sup>4</sup>, Jose M. Cerrato<sup>4</sup>, Kate M. Campbell<sup>5</sup>, Steven B. Yabusaki<sup>6</sup>, Philip E. Long<sup>6</sup>, Rizlan Bernier-Latmani<sup>2</sup>, Daniel E. Giammar<sup>4</sup>, John R. Bargar<sup>3</sup>

<sup>1</sup> Present affiliation: BGD Soil and Groundwater Laboratory, a company of GICON Group, Tiergartenstr. 48, 01219 Dresden, Germany, kulrich@bgd-gmbh.de; <sup>2</sup> Environmental Microbiology Laboratory, École Polytechnique Fédérale de Lausanne, Switzerland; <sup>3</sup> Stanford Synchrotron Radiation Lightsource, Menlo Park, CA, USA; <sup>4</sup> Dept. of Energy, Environmental & Chemical Engineering, Washington University, St. Louis, MO, USA; <sup>5</sup> US Geological Survey, Boulder, CO, USA; <sup>6</sup> Pacific Northwest National Laboratory, Richland, WA, USA; <sup>7</sup> Dept. of Geosciences, Virginia Tech, Blacksburg, VA, USA; <sup>8</sup> School of Physical Sciences, University of Kent, Canterbury, UK; <sup>9</sup> Environmental Science and Engineering, Colorado School of Mines, Golden, CO, USA

**Abstract** In situ bioremediation of uranium-contaminated aquifers through microbially catalyzed reduction of mobile U(VI) species can only be successful if the U(IV) products are immobilized over long time-scales. Although uraninite is known for its low solubility and has been produced in nano-particulate form by several species of metal- and sulfate-reducing bacteria in laboratory studies, little is known about the stability of biogenic U(IV) in the subsurface. Using an up-scaling approach, we investigated the chemical and environmental stability of biogenic UO<sub>2</sub> nano-solids. Our results show that diffusive limitations due to aquifer porosity and microstructure may retard uraninite corrosion. Corrosion was also retarded by adsorption or incorporation of manganese. On the other hand, U(VI) bioreduction in field sediments generated U(IV) that was more labile than biogenic UO<sub>2</sub>.

**Key Words** uraninite, groundwater incubation, dissolution rate, corrosion mechanism, up-scaling

### Introduction

Bioremediation of aquifers contaminated with uranium (U) from abandoned mining or milling sites intends to immobilize dissolved U(VI) in situ through stimulated microbial reduction to a sparingly soluble U(IV) solid. The rationale behind this technique is the persistence of uraninite in low-temperature sedimentary ore deposits formed under reducing conditions. Recent research has shown that microbial U(VI) reduction leads to nano-sized (2–5 nm) particles suggesting enhanced solubility as a result of a proportionally high surface area. Furthermore, detailed knowledge of the molecular structure of the U(IV) phases and responses to varying geochemical conditions is needed. Unfortunately, the isolation of sufficient U(IV) bioreduction products from the field to apply spectroscopic analyses and perform chemical experiments remains a challenge.

We applied an up-scaling approach. First, we characterized biomass-free nano-uraninite produced by *Shewanella oneidensis* MR-1 and determined the intrinsic solubility and dissolution behavior of these products by controlled laboratory experiments (using stirred batch and continuous-flow reactors). Mn(II)-doped biogenic uraninite was studied for comparison because structural incorporation of Mn(II) was expected to reduce the susceptibility to corrosion. Uraninites produced by a variety of different bacterial strains

were then compared to the product characterized for *S. oneidensis* MR-1.

Second, column experiments tested whether similar nano-uraninite accumulated if sediment from a field site (Old Rifle IFRC, Colorado) was augmented with biostimulated *S. oneidensis* cultures. The stability of the formed product was then determined in the presence of artificial Rifle groundwater. In a third step, the reactivity of biogenic nano-uraninite was tested in situ by extended exposure in two Rifle aquifer redox zones. A new encapsulation technology was applied to enable the recapture of the nano-solids for further characterization. This conference paper gives an overview of the major milestones of the collaborative work from the past five years.

### Methods

Methods to determine the stability of biogenic UO<sub>2</sub> followed an up-scaling approach in terms of biogeochemical complexity and instrumental scale from simple bench experiments using stirred batch (SBR) and continuous-flow tank reactors (CFR) to continuous-flow sediment columns (CFC) to field tests where UO<sub>2</sub> nano-solids were exposed in two aquifers by a new encapsulation technology that enabled the recapture of the test solids for further characterization. First, the solubility and dissolution kinetics of NaOH-treated, biomass-free bio-UO<sub>2</sub> and chemogenic uraninite

were compared in simple lab matrices, starting with anoxic HEPES-buffered pure water, followed by an addition of 1 mM NaHCO<sub>3</sub>, followed by additional supply of ≈ 0.5 mg/L dissolved oxygen (DO), finally switched to air-equilibrated water (≈ 9 mg/L DO). The detailed protocols including the synthesis of chemogenic and biogenic UO<sub>2</sub> and the dissolution rate calculation are given in Ulrich *et al.* (2008, 2009).

Second, the form and stability of uranium reduced under biostimulated conditions in sediment derived from a former U-processing site at Old Rifle, CO, were investigated using two bioactive and one bio-suppressed CFC. The sediment was initially augmented with *Shewanella oneidensis* MR-1 and continuously fed with 15 mM lactate and 55 dissolution in the above-mentioned lab matrices and in artificial Rifle groundwater using the CFR technique. For further details refer to Sharp *et al.* (2011).

Finally, NaOH-treated (biomass-free) bio-UO<sub>2</sub> and bio-UO<sub>2</sub> within an intact biomass matrix were exposed in Rifle groundwater by testing two encapsulation techniques, (i) permeable membrane cells constructed from 2 mL polyethylene tubes loaded with uraninite-water suspensions, and (ii) uraninite-doped polyacrylamide gel pucks wrapped in dialysis membranes. The diffusion of water and solutes through a gel puck is expected to be on the order of hours for a 2–3 mm gel (Campbell *et al.* 2007). The tubes were secured in a plastic holder that was deployed at least 1 m below the water table in two different wells, B-02 (a moderately oxidic background well), and P-103 (located in a naturally anoxic zone). Two experi-

ments were carried out that lasted 83 and 102 days. Details on sample characterization and dissolution rate calculation are given in Campbell *et al.* (2011).

**Results and Discussion**

**Bench-scale Studies**

**Carbonate accelerates dissolution of biogenic UO<sub>2</sub> more than of chemogenic UO<sub>2</sub>** Under anoxic conditions, chemogenic UO<sub>2</sub> and cleaned bio-UO<sub>2</sub> (prepared at pH 6.3) showed similar equilibrium solubility (≈ 10<sup>-8</sup> M) and surface area-normalized dissolution rate constants in pure water buffered at around pH 3.3–5.5 · 10<sup>-13</sup> mol U m<sup>-2</sup> s<sup>-1</sup>) (Ulrich *et al.* 2008). This finding is consistent with the structural homology of bio-UO<sub>2</sub> and stoichiometric UO<sub>2.00</sub> (Schofield *et al.* 2008, Bargar *et al.* 2008). However, in the presence of 1 mM NaHCO<sub>3</sub>, the dissolution rates increased for both UO<sub>2</sub> materials, and the biogenic nano-solids yielded higher dissolution rates (1.8 · 10<sup>-10</sup> mol U m<sup>-2</sup> s<sup>-1</sup>) than the chemogenic UO<sub>2</sub> (2.7 · 10<sup>-11</sup> mol U m<sup>-2</sup> s<sup>-1</sup>). While in an anoxic system the presence of carbonate should not significantly alter the solubility of UO<sub>2(am)</sub> (Guillaumont *et al.* 2003), the prompt increase of the dissolution rate in response to the carbonate supply points to faster detachment of oxidized uranium species presumed to have accumulated on the UO<sub>2</sub> surface.

Carbonate also promoted uraninite dissolution under moderately oxidizing conditions. X-ray photoelectron spectroscopy (XPS) detected a higher proportion of U(V) on the bio-UO<sub>2</sub> surface (Ulrich *et al.* 2009). The observed increase of the dissolution rates can be explained by carbonate

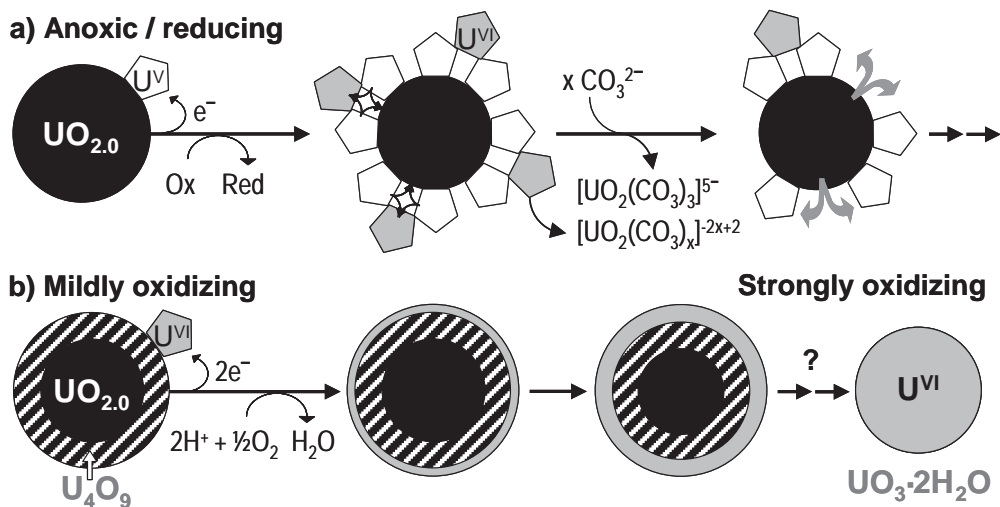


Figure 1 Schematic of UO<sub>2</sub> dissolution under (a) anoxic and (b) mildly to strongly oxidizing conditions. Balls represent particles, white and grey pentagons U(V) and U(VI) ions attached to the UO<sub>2</sub> surface

complexation of U(V) facilitating the detachment of U(V) ions from the surface (Fig. 2.0 to  $UO_{2+x}$ ).

In equilibrium with air, combined spectroscopic results suggest the formation of a near-surface layer of approximate composition  $UO_{2.25}$  ( $U_4O_9$ ) coated by an outer layer of U(VI). This result is in accordance with CFR experiments that indicate control of the dissolution rate of surface-oxidized bio- $UO_2$  by the solubility of the U(VI) oxyhydroxide metaschoepite under the tested condition. While in anoxic systems the dissolution rate will be controlled by the rate of surface oxidation of any trace oxidants (e.g., non-measurable traces of oxygen or reaction products from  $\alpha$ -radiolysis), with increased DO supply the detachment of U(VI) from the surface coating (ultimately oxidized to metaschoepite) will increasingly become the rate-limiting step in the dissolution process (Fig. 1b).

**Manganese incorporation makes biogenic  $UO_2$  more resistant to oxidation** Mn(II), a common groundwater cation, has an ionic radius comparable to that of U(IV) making it suitable for substitution reactions within metal oxides including  $UO_2$ . Because sedimentary uraninites abundantly contain cation impurities that enhance their resistance to oxidation (Janeczek & Ewing 1992, Finch & Ewing 1992), we tested the hypothesis that Mn(II) incorporation into the lattice of bio- $UO_2$  would lower its solubility. The reduction of U(VI) by *S. oneidensis* MR-1 was carried out in the presence of different concentrations of  $MnCl_2$ . Interestingly, high  $Mn^{2+}$  concentrations (up to 8 effect of  $Ca^{2+}$  (Brooks *et al.* 2003). Mn(II)-reacted, biomass-free bio- $UO_2$  had Mn(II) that was both adsorbed and incorporated.

Equilibrium solubility and dissolution kinetics were determined for Mn-reacted bio- $UO_2$  and compared with the results obtained for Mn-free bio- $UO_2$  from SBR and CFR experiments. Under anoxic conditions, the equilibrium uranium concentration was lower for the Mn-reacted bio- $UO_2$  ( $5.5 \cdot 10^{-9}$  M) than for the Mn-free bio- $UO_2$  ( $9.5 \cdot 10^{-9}$  M), which demonstrates a lower solubility for the Mn-reacted nano-solid despite smaller particle size. For the same anaerobic conditions, both materials (Mn-free and Mn-reacted bio- $UO_2$ ) yielded average dissolution rates of  $3.3 \cdot 10^{-13}$  and  $1.2 \cdot 10^{-14}$  mol  $U\ m^{-2}\ s^{-1}$ , versus  $1.0 \cdot 10^{-9}$  and  $2.6 \cdot 10^{-11}$  mol  $U\ m^{-2}\ s^{-1}$  under aerobic conditions, in a carbonate-buffered matrix (1 mM  $NaHCO_3$ ). Thus, the stability of Mn-reacted bio- $UO_2$  is higher than that of Mn-free bio- $UO_2$  by a factor of 28 and 38 (Veeramani *et al.* 2009). The Mn and U analyses in CFR effluent showed that over the duration of the experiment (90 residence times), only  $\approx 18\%$  of the adsorbed Mn(II) was removed, while less than 1% of the total uraninite was dissolved during that time. Hence sorbed or incorporated Mn(II) con-

tributed to the stability of Mn-reacted bio- $UO_2$ .

After removing the adsorbed fraction by repeated pH 5 washes, Mn(II) remained incorporated with 3.0–4.4 wt% (15–21 mol%) of uraninite (Veeramani *et al.* 2009). The divalent oxidation state of incorporated manganese was confirmed by Mn-XANES. Combined results from Mn K-edge EXAFS and U L<sub>III</sub>-edge EXAFS indicated that Mn(II) and U(IV) shared a similar local coordination environment suggesting that Mn(II) occupied U(IV) sites within the  $UO_2$  crystal structure. HRTEM images showed that the average particle size decreased from 2.5 to 1.7 nm ( $\pm 0.15$ ) at the higher Mn concentrations (Veeramani *et al.* 2009). Overall, the results suggest that biogenic uraninite with adsorbed and incorporated Mn(II) is more resistant to oxidation than Mn-free bio- $UO_2$  due to greater thermodynamic stability and slower rates of surface-mediated processes (Veeramani *et al.* 2009). An important constraint for this effect is the absence of Mn(II) oxidizing bacteria or spores that catalyze the oxidation of  $Mn^{2+}$  to  $MnO_2$ , because previous work has shown that biogenic  $MnO_2$  is an effective oxidant for biogenic uraninite (Chinni *et al.* 2008).

**Diverse bacterial strains produce similar nanoparticulate uraninite** Under similar lab conditions, phylogenetically and metabolically diverse strains of dissimilatory metal- and sulfate-reducing bacteria formed biogenic uraninite with particle diameters of 2–3 nm and lattice constants consistent with  $UO_{2.0}$ . Although U(VI) reduction rates were different, structurally similar solids have been obtained with different genera of *Shewanella*, *Anaeromyxobacter*, *Geobacter*, and *Desulfovibrio* (Sharp *et al.* 2009). Given the structural similarities, it is likely that each of these biogenic uraninites have similar properties with regard to stability and can be modeled using the dissolution constants described earlier for biogenic  $UO_2$  product from *Shewanella* sp.

#### **Column-scale Study: Biostimulated U(VI) reduction formed U(IV) phases other than $UO_2$**

Uranium(VI) continuously fed to columns loaded with Rifle sediment was most effectively retained near the inflow section ( $\approx 250$ g sediment). XAS analysis indicated tetravalent uranium lacking the spectroscopic signatures representative of U-U associations within the crystalline  $UO_2$  structure. Consistent with the biogeochemical conditions it is possible to explain the spectra by uranium association with phosphoryl moieties found in biomass, which would imply direct enzymatic U(VI) reduction (Bernier-Latmani *et al.* 2010, Fletcher *et al.* 2010, Sharp *et al.* 2011).

Despite initial augmentation of the sediment with *S. oneidensis*, indigenous bacteria of the phylum Firmicutes dominated the columns just after

11 days and throughout the experiment. After the uranium reduction phase, two months of in situ exposure to oxic,  $30_3$  influent did not result in significant uranium remobilization nor oxygen breakthrough (Sharp *et al.* 2011).

Using the same influent composition, a CFR experiment was applied on the sediment from the inflow section of the biostimulated column to investigate the stability of the unknown U(IV) phase at a solids concentration of  $\approx 8.5$  g/L (substantially lower than in the columns and during in situ exposure). The best match to the U-release curve was obtained by calculations assuming two pools of solid U phases releasing U simultaneously at two different rates. A smaller pool of initially 29% of total U showed a higher release rate of  $(5.5 \pm 0.6) \cdot 10^{-5}$  mol (g U) $^{-1}$  s $^{-1}$  whereas the other 71% of the total U exhibited a lower release rate of  $(8.1 \pm 0.9) \cdot 10^{-7}$  mol (g U) $^{-1}$  s $^{-1}$ . Because complementary digestions and structural analyses showed that the fraction of U(VI) in the sediment was very small, and XAS data ruled out significant  $UO_2$  in the sediment, these findings suggest the presence of two different forms of U(IV) in the sediment with different physical release mechanisms or oxidation rates (Sharp *et al.* 2011).

The U release rate of the less labile, predominant U-phase in air-equilibrated water containing 30 mM  $NaHCO_3$  was 4-times higher than for bio- $UO_2$  under similar experimental conditions. Under reducing and carbonate-free conditions, the measured U release rate from the sediment of  $1.4 \cdot 10^{-8}$  mol (g U) $^{-1}$  s $^{-1}$  was 5 orders of magnitude higher than for bio- $UO_2$  dissolution ( $5.3 \cdot 10^{-13}$  mol (g U) $^{-1}$  s $^{-1}$ ). While these calculated rates include the effects of physical transport processes such as diffusion of oxygen and carbonate into micropores of the bulk sediment and diffusion of desorbed U(IV) or oxidized U(VI) out of such pores, they represent an upper bound for uranium mobility at a solids concentration of  $\approx 8.5$  g/L and verify that the U(IV) phases obtained are less stable under both anoxic and oxic conditions than were the investigated biomass-free bio- $UO_2$  solids (Ulrich *et al.* 2009).

#### **Field-scale Study: Diffusion-driven transport lagged corrosion of incubated biogenic $UO_2$**

During the 102-day incubation period in the moderately oxic well B-02, 55% of the initial mass of NaOH-treated bio- $UO_2$  was lost by dissolution as compared to 11% mass loss for the biomass-associated  $UO_2$ . Because the biomass should not provide a significant redox buffer nor was it metabolically active, the difference in stability is more likely due to retarded diffusion of DO to the uraninite surface and of desorbed U(VI) into the aquifer (Campbell *et al.* 2011).

XAS analyses showed that U(VI) minerals did

not accumulate during in-well deployment, and the uraninite unit cell structure was not substantially altered by interaction with groundwater. Thus, a faster oxidation of surface U(IV) atoms relative to the detachment of the oxidized surface species, leading to accumulation of U(VI) solids (Fig. 1b), can be ruled out. In contrast, the relative abundance of bicarbonate (2–3 mM) in combination with  $< 2$  mg/L DO may enable oxidized surface U(VI) atoms to be removed more rapidly than they accumulate (Fig. 1a), suggesting that oxidation of the uraninite surface is the rate-limiting step in the dissolution process. Because the overall rate of  $UO_2$  dissolution was approximately two orders of magnitude lower than predicted based on CFR results, a reactive transport model was applied to estimate the effect of transmembrane diffusion of DO and U(VI) on the overall loss rates under the given groundwater conditions of well B-02.

While the observed loss of 3–5 mg of cleaned bio- $UO_2$  from the gel pucks is consistent with the model prediction ( $\approx 3$  mg loss over the 102-day incubation period), an additional sensitivity analysis indicated that diffusion is a key control on the rate of uraninite dissolution in the system. Although natural bio- $UO_2$  would not be secured by diffusion-limiting membranes or gels, a spectrum of other diffusion limiting conditions can be expected in aquifers, including pore size and shape, particle size, porosity, and diffusivity, in particular in low conductivity flow regimes. In fine-grained sediments (such as those common in naturally bio-reduced zones), the presence of diffusive barriers should be expected to profoundly impact U oxidation. Precipitation of iron sulfides and calcite and accumulation of biomass during biostimulation are expected to decrease sediment permeability, which would augment the redox buffering capacity of iron sulfides with a diffusive effect (Campbell *et al.* 2011).

#### **Conclusions**

It has been hypothesized that the oxidation of bio- $UO_2$  in aquifers would proceed faster than that of bulk uraninite because of its nanoparticulate nature (Wall & Krumholz 2006). Although we found similar intrinsic solubility and dissolution rates of bio- $UO_2$  nano-solids and bulk  $UO_2$  in pure anoxic water, groundwater solutes can also affect the stability of bio- $UO_2$ . While carbonate and protons (Ulrich *et al.* 2008) accelerated the dissolution of bio- $UO_2$  even more than of chemogenic  $UO_2$ ,  $Mn^{2+}$  impeded these reactions by surface adsorption and / or structural incorporation.

Through up-scaling from simple lab systems to complex field substrates, we learned that microbial communities can rapidly shift and produce other forms of bio-reduced U(IV) that are less stable than bio- $UO_2$ . Moreover, the microstructure of

soils and sediments as well as association of U(IV) with biomass can limit diffusion of DO and groundwater solutes. Hence, physical transport can become rate-limiting for the oxidation and dissolution of biogenic UO<sub>2</sub> nano-solids in the subsurface. Collectively, results presented here and elsewhere (Bernier-Latmani *et al.* 2010, Fletcher *et al.* 2010, Sivaswamy *et al.* 2011, Ulrich *et al.* 2011, Veeramani *et al.* 2011) emphasize the role of the geochemical environment in both formation and intrinsic stability of biogenic U(IV) products.

### Acknowledgements

We thank Eugene Ilton for the XPS study. Work at WUSTL was partially supported by the U.S. Department of Energy (Grant DE-FG02-06ER64227). Work carried out at EPFL was funded by Swiss NSF grant No. 20021-113784, SNSF International Co-operation grant No. IZKOZ2-12355, and DOE OBER grant No. DE-FG02-06ER64227. Portions of this research were carried out at the Stanford Synchrotron Radiation Lightsources, a national user facility operated by Stanford University on behalf of the U.S. Department of Energy (DOE), Office of Basic Energy Sciences and supported by the SSRL Environmental Remediation Science Program and BER-ERSD project number SCW0041. The SSRL Structural Molecular Biology Program is supported by the Department of Energy, Office of Biological and Environmental Research, and by the National Institutes of Health, National Center for Research Resources, Biomedical Technology Program.

### References

- Bargar JR, Bernier-Latmani R, Giammar DE, Tebo BM (2008) Biogenic uraninite nanoparticles and their importance for uranium remediation. *Elements* 4(6):407–412
- Bernier-Latmani R, Veeramani H, Vecchia ED, Junier P, Lezama-Pacheco JS, Suvorova E, Sharp JO, Wigginton NS, Bargar JR (2010) Non-uraninite products of microbial U(VI) reduction. *Environ Sci Technol* 44:5104–5111
- Brooks SC, Fredrickson JK, Carroll SL, Kennedy DW, Zachara JM, Plymale AE, Kelly SD, Kemner KM, Fendorf S (2003) Inhibition of bacterial U(VI) reduction by calcium. *Environ Sci Technol* 37(9):1850–1858
- Campbell KM, Root R, O'Day PA, Hering JG (2007) A gel probe equilibrium sampler for measuring arsenic porewater profiles and sorption gradients in sediments: I. Laboratory development. *Environ Sci Technol* 42:497–503
- Campbell KM, Veeramani H, Ulrich KU, Blue LY, Giammar DE, Bernier-Latmani R, Stubbs JE, Suvorova E, Yabusaki S, Lezama-Pacheco JS, Mehta A, Long PE, Bargar JR (2011) Oxidative dissolution of biogenic uraninite in groundwater at Old Rifle, CO. *Environ Sci Technol* (revision resubmitted)
- Chinni S, Anderson CR, Ulrich KU, Giammar DE, Tebo BM (2008) Indirect UO<sub>2</sub> oxidation by Mn(II)-oxidizing spores of *Bacillus* sp strain SG-1 and the effect of U and Mn concentrations. *Environ Sci Technol* 42(23): 8709–8714
- Finch RJ, Ewing RC (1992) The corrosion of uraninite under oxidizing conditions. *J Nucl Mater* 190:133–156
- Fletcher KE, Boyanov MI, Thomas SH, Wu Q, Kemner KM, Löffler FE (2010) U(VI) reduction to mononuclear U(IV) by desulfitobacterium species. *Environ Sci Technol* 44(12):4705–4709
- Guillaumont R, Fanghänel T, Fuger J, Grenthe I, Neck V, Palmer DA, Rand MH (2003) Update on the chemical thermodynamics of uranium, neptunium, plutonium, americium and technetium. OECD Nuclear Energy Agency, Elsevier Amsterdam
- Janeczek J, Ewing RC (1992) Structural formula of uraninite. *J Nucl Mater* 190:128–132
- Schofield EJ, Veeramani H, Sharp JO, Suvorova E, Bernier-Latmani R, Mehta A, Stahlman J, Webb SM, Clark DL, Conradson SD, Ilton ES, Bargar JR (2008) Structure of biogenic uraninite produced by *Shewanella oneidensis* strain MR-1. *Environ Sci Technol* 42(21):7898–7904
- Sharp JO, Schofield EJ, Veeramani H, Suvorova EI, Kennedy DW, Marshall MJ, Mehta A, Bargar JR, Bernier-Latmani R (2009) Structural similarities between biogenic uraninites produced by phylogenetically and metabolically diverse bacteria. *Environ Sci Technol* 43(21):8295–8301
- Sharp JO, Lezama-Pacheco JS, Schofield EJ, Junier P, Ulrich KU, Chinni S, Veeramani H, Margot-Roquier C, Webb SM, Tebo BM, Giammar DE, Bargar JR, Bernier-Latmani R (2011) Uranium speciation and stability after reductive immobilization in aquifer sediments. *Geochim Cosmochim Acta* (revision resubmitted)
- Sivaswamy V, Boyanov MI, Peyton BM, Viamajala S, Gerlach R, Apel WA, Sani RK, Dohnalkova A, Kemner KM, Borch T (2011) Multiple mechanisms of uranium immobilization by *Cellulomonas* sp. strain ES6. *Biotechnol Bioeng* 108(2):264–276
- Ulrich KU, Singh A, Schofield EJ, Bargar JR, Veeramani H, Sharp JO, Bernier-Latmani R, Giammar DE (2008) Dissolution of biogenic and synthetic UO<sub>2</sub> under varied reducing conditions. *Environ Sci Technol* 42(15): 5600–5606
- Ulrich KU, Ilton ES, Veeramani H, Sharp JO, Bernier-Latmani R, Schofield EJ, Bargar JR, Giammar DE (2009) Comparative dissolution kinetics of biogenic and chemogenic uraninite under oxidizing conditions in the presence of carbonate. *Geochim Cosmochim Acta* 73(20):6065–6083
- Ulrich KU, Veeramani H, Bernier-Latmani R, Giammar DE (2011) Speciation-dependent kinetics of uranium (VI) bioreduction. *Geomicrobiol J*: in press

Veeramani H, Schofield EJ, Sharp JO, Suvorova EI, Ulrich KU, Mehta A, Giammar DE, Bargar JR, Bernier-Latmani R (2009) Effect of Mn(II) on the structure and reactivity of biogenic uraninite. *Environ Sci Technol* 43(17):6541–6547

Veeramani H, Alessi D, Suvorova E, Lezama-Pacheco J, Stubbs J, Sharp J, Dippon U, Kappler A, Bargar JR,

Bernier-Latmani R (2011) Products of abiotic U(VI) reduction by biogenic magnetite and vivianite. *Geochim Cosmochim Acta* 75(9):2512–2528

Wall JD, Krumholz LR (2006) Uranium reduction. *Ann Rev Microbiol* 60:149–166